the FEBS Journal

Onconase cytotoxicity relies on the distribution of its positive charge

Rebecca F. Turcotte[1], Luke D. Lavis[2] and Ronald T. Raines[2,3]

1 Medical Scientist Training Program and Biophysics Graduate Program, University of Wisconsin–Madison, WI, USA
2 Department of Chemistry, University of Wisconsin–Madison, WI, USA
3 Department of Biochemistry, University of Wisconsin–Madison, WI, USA

Keywords
cancer; Coulombic interaction; cytotoxin; enzyme; ribonuclease

Correspondence
R. T. Raines, Department of Biochemistry, University of Wisconsin–Madison, 433 Babcock Drive, Madison, WI 53706-1544, USA
Fax: +1 608 890 2583
Tel: +1 608 262 8588
E-mail: rtraines@wisc.edu
Website: http://www2.biochem.wisc.edu/raines

(Received 15 December 2008, revised 7 May 2009, accepted 14 May 2009)

doi:10.1111/j.1742-4658.2009.07098.x

Onconase® (ONC) is a member of the ribonuclease A superfamily that is toxic to cancer cells *in vitro* and *in vivo*. ONC is now in Phase IIIb clinical trials for the treatment of malignant mesothelioma. Internalization of ONC to the cytosol of cancer cells is essential for its cytotoxic activity, despite the apparent absence of a cell-surface receptor protein. Endocytosis and cytotoxicity do, however, appear to correlate with the net positive charge of ribonucleases. To dissect the contribution made by the endogenous arginine and lysine residues of ONC to its cytotoxicity, 22 variants were created in which cationic residues were replaced with alanine. Variants with the same net charge (+2 to +5) as well as equivalent catalytic activity and conformational stability were found to exhibit large (> 10-fold) differences in toxicity for the cells of a human leukemia line. In addition, a more cationic ONC variant could be either much more or much less cytotoxic than a less cationic variant, again depending on the distribution of its cationic residues. The endocytosis of variants with widely divergent cytotoxic activity was quantified by flow cytometry using a small-molecule fluorogenic label, and was found to vary by twofold or less. This small difference in endocytosis did not account for the large difference in cytotoxicity, implicating the distribution of cationic residues as being critical for lipid-bilayer translocation subsequent to endocytosis. This finding has fundamental implications for understanding the interaction of ribonucleases and other proteins with mammalian cells.

Introduction

Several homologues and variants of bovine pancreatic ribonuclease (RNase A) [1,2] exhibit antitumoral activity [3–7]. The molecular basis for this extraordinary attribute is under intense scrutiny in several laboratories [8]. These efforts are providing many insights; for example, cytotoxic ribonucleases are known to catalyze the degradation of RNA [9,10], even in the presence of the mammalian ribonuclease inhibitor protein (RI) [11], which binds to RNase A and mammalian homologues with nearly femtomolar affinity [12–15]. Cytotoxic ribonucleases have high conformational stability and resistance to proteolysis [16–19]. Lastly, cytotoxic ribonucleases enter the cytosol of cells [20], a remarkable feat that appears to correlate with net positive charge [21,22].

Onconase® (ONC) [23,24], an RNase A homologue from the northern leopard frog *Rana pipiens*, is toxic to tumor cells both *in vitro* and *in vivo* [25,26]; cells

Abbreviations
6-FAM, 6-carboxyfluorescein; ONC, Onconase® (a registered trademark of Alfacell Corp.) or ranpirnase; RI, mammalian ribonuclease inhibitor; RNase A, bovine pancreatic ribonuclease; RNase 1, human pancreatic ribonuclease; 6-TAMRA, 6-carboxytetramethylrhodamine; TML, trimethyl lock; *Z*, net molecular charge: Arg + Lys – Asp – Glu.

exposed to ONC die via apoptosis [27–29]. A Phase IIIb clinical trial of ONC in combination with doxorubicin for the treatment of malignant mesothelioma is nearing completion [30,31], and ONC is on the verge of approval as a second-line chemotherapeutic agent. Side effects of ONC treatment include dose-limiting renal toxicity that is reversible upon discontinuation of the drug [30]. Surprisingly, the allergic response is minimal, even following repeated infusions, an attribute that might result from an increase in activation-induced apoptosis of lymphocytes exposed to ONC [32].

ONC is a single-domain protein with 104 amino acid residues and a molecular mass of 11.8 kDa (Fig. 1A) [9]. Its two-lobed structure is characteristic of the ribonuclease A superfamily (Fig. 1B, C). Two lysine residues, Lys9 and Lys31, stabilize the transition state during cleavage of an RNA substrate [33]. The N-terminal residue of ONC is an unusual pyroglutamate that forms a hydrogen bond with Lys9, positioning it properly for catalysis [33,34].

The physicochemical attributes of ONC suggest why it is an especially efficacious cytotoxin. First, ONC does not interact with RI under physiological conditions [35,36]. Second, ONC has extreme conformational stability ($T_m \sim 90$ °C) [19,37]. Third, ONC is a highly basic protein ($Z = +5$; p$I > 9.5$) [9], an attribute that is important for the catalysis of RNA cleavage [33,38–41] and might facilitate cytosolic entry [21,42,43].

Several lines of evidence suggest that cytosolic entry limits the cytotoxicity of ONC. For example, ONC is more toxic when injected directly into cells [44], or when internalization is aided by either lipofection [27] or conjugation to a targeting antibody [45,46]. Other protein toxins, such as Shiga toxin, cholera toxin and ricin, contain two domains, one that binds to the cell surface and another that exerts a toxic effect in the cytosol [47]. ONC differs in that its single domain accomplishes both cytosolic entry and cytotoxicity.

No cell-surface receptor for ONC has been identified to date [48–50]. The binding of ONC to HeLa cells in culture is not saturable at ONC concentrations (≤ 10 μM) that far exceed its lethal dose [50]. The different composition of the surface of cancer cells compared with that of normal cells might target ribonucleases selectively to cancer cells [4,6,50], thereby contributing to the favorable therapeutic index that has been observed in animal models and human trials [26,31]. For example, the surface of cancer cells exhibits major changes in heparan sulfate glycosaminoglycan profile [51], phospholipid composition [52,53] and ganglioside display [54].

Internalization of ONC is an energy-dependent process, and acidification of endosomes is not a requirement for cytosolic entry [48,50]. Indeed, studies on purified endosomes suggest that increasing endosomal pH (toward neutrality) actually increases translocation [55]. The effects of drugs that alter Golgi trafficking suggest that this route is not a productive one for ONC-mediated cytotoxicity [48–50]. Recent work suggests that ONC enters cells via AP2/clathrin-mediated endocytosis, followed by routing through recycling endosomes [55]. These studies on the internalization of ONC should be interpreted with caution, however, because treatment with small-molecule drugs and metabolic inhibitors can have diverse effects on cellular trafficking. Studies in a HeLa cell line overexpressing a dominant-negative mutant of dynamin suggest that ONC internalization does not occur via a dynamin-dependent endocytic pathway [50].

The cytotoxicity of ribonucleases seems to correlate with their net positive charge [21,22]. Specifically, adding positive charge via site-directed mutagenesis [56,57], appending protein transduction domains [58] and chemical modification [42,59] enhances the cytotoxicity of toxic or nontoxic ribonucleases. Rigorous interpretation of these results is confounded, however, by concurrent changes in the affinity for RI and by the heterogeneity of chemically modified proteins [42].

Because ONC does not have a measurable affinity for RI, we reasoned that it was the ideal RNase A homologue for a thorough dissection of the contribution of its positive charge to its cytotoxicity. Here, we report on the results of such a dissection – based on the systematic alteration of the three arginine and twelve lysine residues of wild-type ONC, few of which are conserved in RNase A (Fig. 1A). We find that the net charge of an ONC variant has surprisingly little effect on its cytotoxicity. Rather, it is the distribution of that charge which is critical.

Results

Design of ONC variants

ONC contains a total of 15 positively charged residues −3 arginines and 12 lysines (Fig. 1A). An electrostatic potential map of ONC (Fig. 1D, E) reveals three regions other than the active site that contain a high density of positive charge at neutral pH. These 'patches' each contain three positively charged residues. Patch 1 consists of Lys45, Lys49 and Lys55, patch 2 consists of Arg15, Lys80 and Lys81, and patch 3 consists of Arg73, Lys76 and Lys78 (Fig. 1B–E). The remaining six positively charged residues are within the active site (Lys9 and Lys31), proximal to the active site (Lys8 and Lys33) or form small, isolated regions of

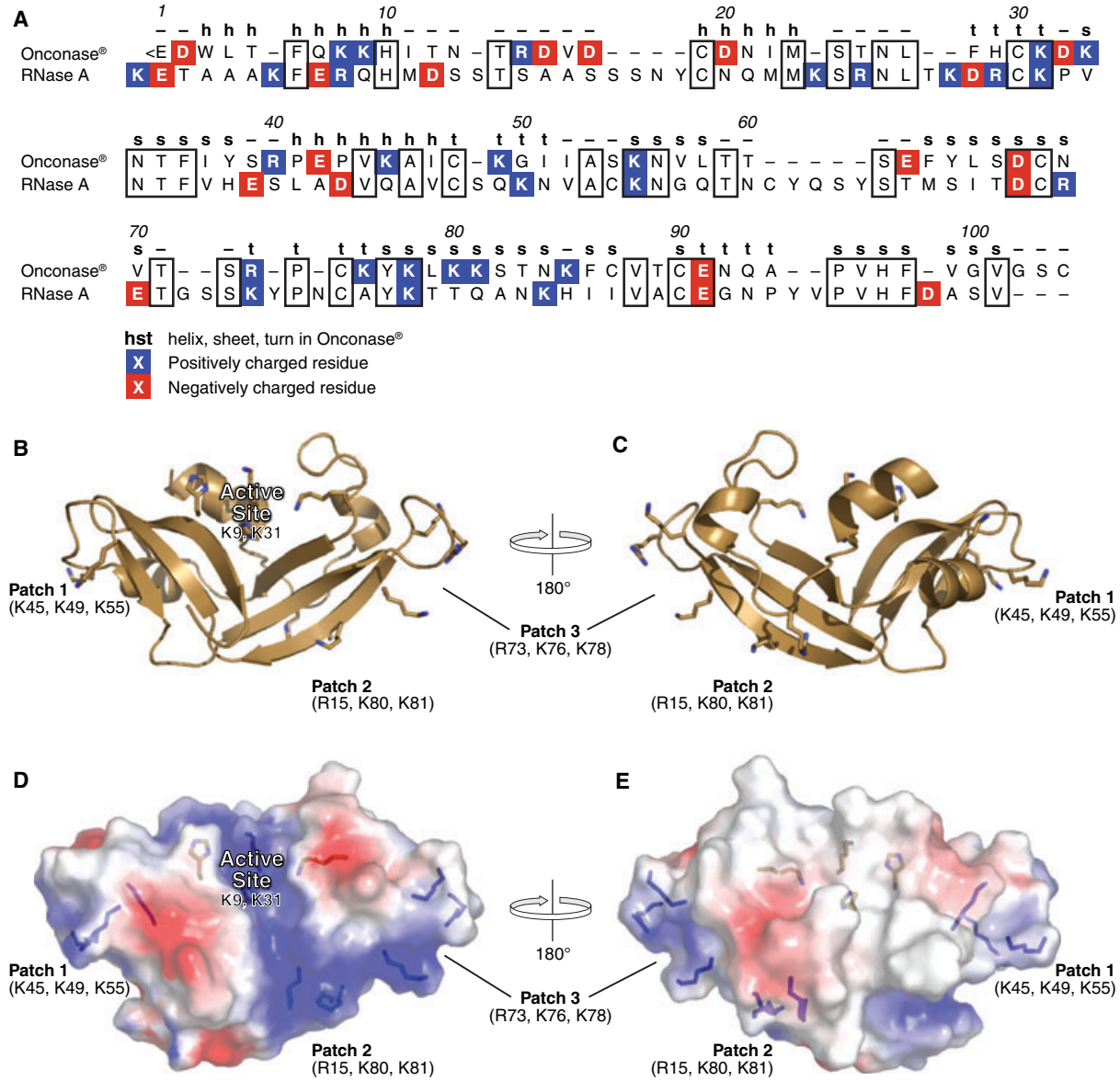

Fig. 1. Amino acid sequence and 3D structure of Onconase (ONC). (A) Amino acid sequence of ONC and its alignment with that of RNase A. Positively charged residues are in a blue box; negatively charged residues are in a red box. (B,C) Cartoon of the 3D structure of ONC (Protein Data Bank entry 1onc) [82]. (D,E) Electrostatic potential map of the ONC surface with positively charged surface in blue, negatively charged surface in red and neutral surface in white. The conventional view of ONC is shown in (B) and (D), and is rotated by 180° in (C) and (E). Images were created using the program MACPYMOL (DeLano Scientific, San Francisco, CA, USA).

positively charged surfaces (Arg40 and Lys85), and thus were not included in this analysis.

We began by replacing all of the arginine and lysine residues within each patch with alanine. If net charge were the key to ONC cytotoxicity, then a variant with three substitutions distributed across the three patches would manifest the same cytotoxicity as the three patch variants. We created such a variant, R15A/K49A/R73A ONC, by replacing the three residues that were at the geometric 'center' of each of the patches (that is, having the shortest distance to the other two residues, as measured from C^{ε} of arginine and N^{ε} of lysine), as well as two other distributed variants, R15A/K45A/K76A ONC and R15A/K55A/K76A ONC.

To test the hypothesis that the detailed structure of the patches is important for cytotoxicity, double-substituted variants were designed and created. These variants had all nine ($= {}_3C_2 \times 3$) of the possible permutations of two residues in the three variants

with abolished cytotoxicity (i.e. R15A/K80A/K81A ONC, R73A/K76A/K78A ONC and R15A/K49A/R73A ONC).

To ascertain the relative importance of residues 15, 73, 76, 78, 80 and 81 from patches 2 and 3 in the cytotoxicity of ONC, each of these residues was replaced individually with alanine. The single variant K49A ONC was also made, prompted by the abolished cytotoxicity of the distributed variant, R15A/K49A/R73A ONC.

Position 61 was chosen for the labeling of ONC variants with a fluorogenic label that enables a quantitative measure of endocytosis. Although the D16C [50] and S72C [55] substitutions had been used previously to label ONC, we preferred to avoid any changes in charge (even negative charge), and also wanted to choose a position remote from the active site and all three patches. Ser61 met both of these criteria, and was replaced with a cysteine residue to create an S61C variant.

All labeled and unlabeled variants were ~ 95% pure according to SDS/PAGE, and the identities of all purified proteins and conjugates were confirmed by MALDI–TOF MS (Table S1).

Cytotoxicity

The three patch variants, K45A/K49A/K55A ONC (patch 1), R15A/K80A/K81A ONC (patch 2) and R73A/K76A/K78A ONC (patch 3), were assayed for toxicity toward K-562 cells, a leukemic cell line (Fig. S1). Wild-type ONC is toxic to K-562 cells with an IC_{50} value of ~ 0.3 μM. K45A/K49A/K55A ONC retained measurable, albeit severely reduced, cytotoxicity (IC_{50} = 8.2 μM). The R15A/K80A/K81A and R73A/K76A/K78A variants, however, lost all measurable cytotoxicity.

The first distributed variant, R15A/K49A/R73A ONC, was not cytotoxic. Two other variants with distributed substitutions, R15A/K45A/K76A ONC and R15A/K55A/K76A ONC, had higher cytotoxicity (Fig. S1).

The double variants can be divided into three subsets based on their cytotoxic activity. Three variants, R15A/K80A, R15A/K81A and R73A/K76A, retain relatively high cytotoxicity (IC_{50} values of 1.5–2.7 μM; Fig. S2); three, K80A/K81A, R15A/K49A and R15A/R73A, possess intermediate cytotoxicity (IC_{50} values of 4.7–6.2 μM; Fig. S2); and three variants, R73A/K78A, K76A/K78A and K49A/R73A, have nearly abolished, but measurable, cytotoxicity (IC_{50} values of 10.5–11.8 μM; Fig. S2).

All of the singly substituted variants of ONC – R15A, K49A, R73A, K76A, K78A, K80A and K81A – had IC_{50} values that were within fivefold of that of wild-type ONC and within error of each other (Table 1). The IC_{50} values for the single, double and triple variants of ONC are depicted together in Fig. 2.

Ribonucleolytic activity

The ability to cleave a fluorogenic tetranucleotide RNA substrate was measured for each ONC variant. All variants had ribonucleolytic activity within fivefold of that of the wild-type enzyme (Table 1). This result indicates that any observed decrease in cytotoxicity was not caused by a decrease in ribonucleolytic activity, which is required for cytotoxicity [60], and that the variants had attained the correct 3D structure, because catalytic activity is an exquisite indicator of native tertiary structure [61].

Table 1. Properties of Onconase (ONC) and its variants. ND, not determined.

ONC	IC_{50}[a] (μM)	k_{cat}/K_M[b] (10^3 $M^{-1}\cdot s^{-1}$)	T_m[c] (°C)
Wild-type	0.3	34 ± 2	83
Patch variants			
K45A/K49A/K55A (*Patch 1*)	8.2	12 ± 1	76
R15A/K80A/K81A (*Patch 2*)	> 25	7.8 ± 0.2	78
R73A/K76A/K78A (*Patch 3*)	> 25	17 ± 1	73
Distributed variants			
R15A/K49A/R73A	> 25	6.5 ± 0.3	82
R15A/K45A/K76A	4.8	12 ± 1	77
R15A/K55A/K76A	2.6	16 ± 1	79
Double variants			
K49A/R73A	11.8	26 ± 9	82
R73A/K78A	11.3	23 ± 2	81
K76A/K78A	10.5	22 ± 1	79
R15A/R73A	6.2	9 ± 1	84
K80A/K81A	5.5	14 ± 2	79
R15A/K49A	4.7	6.6 ± 0.5	83
R73A/K76A	2.7	34 ± 7	ND
R15A/K80A	2.1	11 ± 1	ND
R15A/K81A	1.5	16 ± 4	ND
Single variants			
R15A	1.1	30 ± 10	ND
K49A	0.9	ND	ND
R73A	1.2	28 ± 5	ND
K76A	0.8	33 ± 4	ND
K78A	1.3	30 ± 4	ND
K80A	1.5	22 ± 3	ND
K81A	1.4	21 ± 4	ND

[a] Values of IC_{50} are for the incorporation of [*methyl*-^{3}H]thymidine into DNA of K-562 cells. [b] Values of k_{cat}/K_M (± SE) are for the cleavage of 6-FAM–dArUdGdA–6-TAMRA in 0.10 M Mes/NaOH buffer (pH 6.0) containing 0.10 M NaCl at 23 ± 2 °C. [c] Values of T_m were determined in NaCl/P_i by CD spectroscopy.

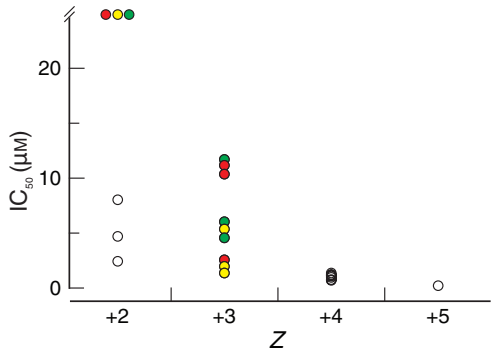

Fig. 2. Effect of wild-type Onconase (ONC) and 22 variants on the proliferation of K-562 cells, as reported by values of IC_{50}. Ribonucleases are sorted by their net molecular charge (Z). A single alanine to arginine/lysine reversion converts a nontoxic variant with $Z = +2$ (R15A/K49A/R73A, green; R15A/K80A/K81A, yellow; R73A/K76A/K78A, red) into a cytotoxic variant with $Z = +3$. Data are listed in Table 1.

Conformational stability

Like ribonucleolytic activity, conformational stability correlates with the cytotoxicity of ribonucleases [17]. Therefore, the decrease in cytotoxicity observed in these variants might have been caused by a decrease in stability. To determine the contribution of this attribute, the values of T_m (the temperature of the midpoint of the denaturation curve) of all of the triple variants and double variants with low or moderate cytotoxicity were measured by thermal denaturation monitored by CD spectroscopy. The T_m values of these variants were similar to those of the wild-type protein, and were >> 37 °C (Table 1). The modest differences in T_m values did not correlate with cytotoxicity.

Endocytosis

Several variants were selected in order to test their ability to enter the endosomes of K-562 cells. Using a strategy based on the trimethyl lock (TML), our laboratory developed a method to observe the endocytosis of proteins in unwashed cells [62,63]. Briefly, a protein is labeled with a fluorogenic label (Fig. 3A) that is unmasked by nonspecific esterases in endosomes or the cytosol. The resulting fluorescence is then quantified by flow cytometry. Using this method, the cellular internalization of wild-type ONC was found to be much less efficient than that of human pancreatic ribonuclease (RNase 1) (Fig. 3B). *In vitro* activation of the labeled ribonucleases with porcine liver esterase revealed a twofold difference in the fluorescence intensity of labeled ONC and RNase 1 (data not shown), which does not account for the > 10-fold difference observed in the flow cytometer.

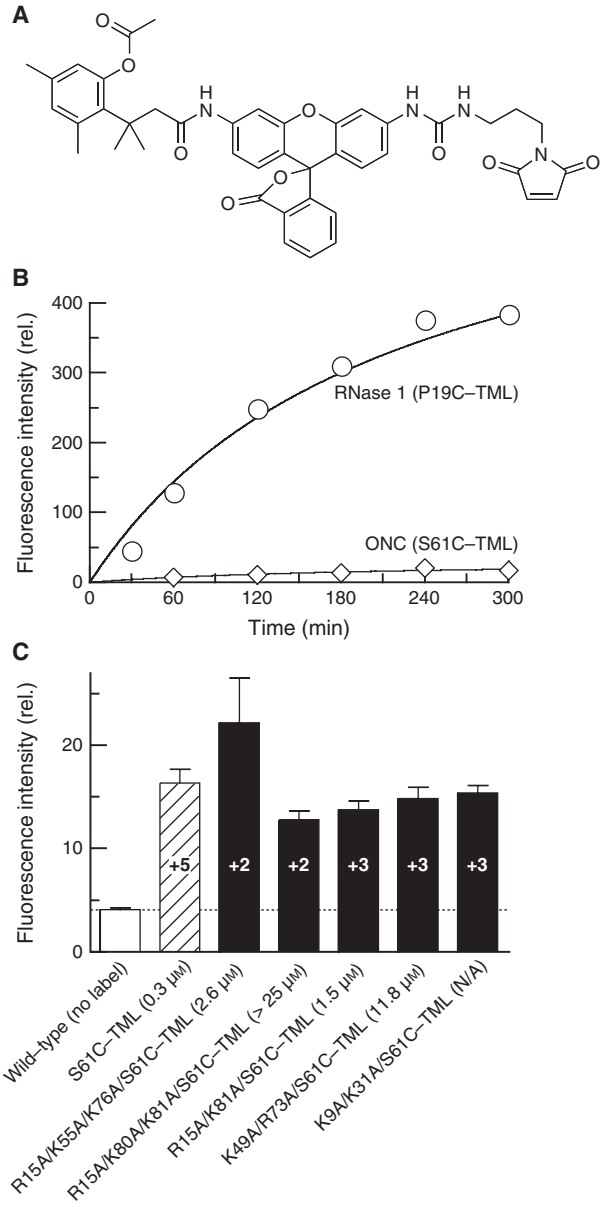

Fig. 3. Internalization of Onconase (ONC), its variants and RNase 1 into K-562 cells. Internalization was measured by using flow cytometry to evaluate the fluorescence manifested by a ribonuclease (10 μM) labeled with a fluorogenic label [62] and incubated with K-562 cells at 37 °C. (A) Structure of the fluorogenic label, which was attached via its maleimido group to Cys61 of S61C ONC and Cys19 of P19C RNase 1. (B) Time course of internalization of ONC and RNase 1 [63]. (C) Relative internalization (± SE) of ONC variants after 4 h. Values of Z are indicated on each bar; values of IC_{50} for the corresponding unlabeled ribonuclease are shown in parentheses. The dashed line indicates the background level of fluorescence, as revealed with unlabeled ONC.

One pair of ONC variants, the triply substituted pair, exhibited a significant difference in their ability to be endocytosed into K-562 cells. R15A/K55A/

K76A/S61C–TML ONC appeared to enter endosomes twice as well as did R15A/K80A/K81A/S61C–TML ONC. The other variants, including K9A/K31A/S61C–TML ONC, differed little from the positive control, S61C–TML ONC (Fig. 3C).

Discussion

ONC is able to kill cancer cells specifically [25,26,31,48], an attribute that is dependent on its ability to enter the cytosol. Much has been learned about this process, but many aspects remain mysterious. For example, the molecular basis for cytosolic entry is unclear. The chemical cationization of other ribonucleases has been shown to increase their cytotoxicity [42,43,56,58], suggesting that positive charge is important for cytosolic entry and, hence, the cytotoxicity of ONC and other ribonucleases. Because ONC does not bind to RI under physiological conditions [35,36], it is an attractive model for the examination of internalization with minimal obfuscation. Accordingly, we set out to delineate the relative importance of various regions of positive charge on the surface of ONC to its cytotoxicity.

Importance of patch 3 (R73/K76/K78) and K49 to cytotoxicity

The replacement of three positively charged patches on the surface of ONC (Fig. 1D, E) resulted in variants with disparate cytotoxic activities, with only the K45/K49/K55 variant (patch 1) retaining measurable cytotoxicity (Table 1 and Fig. S1). This result indicates that charge distribution is critical for the cytotoxicity of ONC, and that patches 2 and 3 are relatively important in this process.

Variants with two substitutions within each patch provided additional insight. The three variants that resulted from patch 2 did not exhibit major changes in cytotoxicity, with two retaining high cytotoxicity and one having moderate cytotoxicity (Fig. 2). Of the three variants from patch 3, however, two had low cytotoxicity and one retained high cytotoxicity. These data, combined with the replacement of each patch in turn (above), suggest that patch 3 is the most important of the three for the cytotoxicity of ONC.

The results for the cytotoxicity of the three variants in which substitutions were distributed among the patches suggest that the detailed character of the three patches is important, because these three variants differed widely in cytotoxic activity (Table 1 and Fig. S1). In an attempt to determine the relative contributions of each residue to the loss of cytotoxicity, all residues in patches 2 and 3, plus residue 49 from the distributed variant with no cytotoxicity, were replaced in turn with alanine. The IC_{50} values for these variants were all within fivefold of that for wild-type ONC (Table 1), indicating that no individual positively charged residue is critical for cytotoxicity. Rather, the cationic residues on ONC appear to act in a degenerate manner, as expected for the manifestation of a nonspecific interaction with anionic membrane components.

To determine if a particular pair of residues is most responsible for internalization and cytotoxicity, we made double substitutions within R15A/K49A/R73A ONC, in addition to the double substitutions from patches 2 and 3 (above). The residues of patch 3 and Lys49 comprise all of the residues whose replacement in the double-substituted variants results in the lowest cytotoxicity (Fig. S2). Indeed, replacement of Lys49 and Arg73 resulted in the largest loss of cytotoxicity in a doubly substituted variant. Interestingly, these residues are 45 Å apart. This result is consistent with multivalent binding of ONC to anionic membrane components, such as the sulfuryl groups of heparan-sulfate proteoglycans and the carboxyl groups of sialic acid-containing gangliosides.

Depicting the cytotoxic activity of wild-type ONC and all 22 variants studied herein as a function of their net molecular charge provides additional insight (Fig. 2). In addition to showing that variants with the same net charge differ in their cytotoxic activity, this portrayal shows clearly that more cationic variants tend to be more cytotoxic, but are not necessarily so. An ONC variant with $Z = +3$ can be either much more cytotoxic or much less cytotoxic than a variant with $Z = +2$, depending on the distribution of its cationic residues. Moreover, when an arginine or lysine residue is added to a particular variant with $Z = +2$ to form a variant with $Z = +3$, the location of that residue determines the cytotoxicity of the resultant variant. Finally, it is apparent that variants of ONC with charges ranging from $+2$ to $+5$ can have marked cytotoxic activity.

Cationic residues do not affect cellular binding and endocytosis

What causes the differences in cytotoxicity that are seen in the alanine-substituted variants of ONC? The current model for the process of cell death for ONC-exposed cells can be divided into four steps (Fig. 4). ONC binds to the cell surface, likely via interactions with negatively charged components of the plasma membrane. Then, bound ONC is internalized via endocytosis. Some ONC escapes from endosomes and

translocates into the cytosol [50,64]. There, ONC cleaves RNA substrates [9,44,65], resulting in cell death by apoptosis [27–29]. An additional requirement for cytotoxicity is that ONC and other cytotoxic ribonucleases be active catalysts at physiological temperature and not be susceptible to proteolysis [17].

The large differences among the ONC variants in their ability to kill cancer cells, combined with the small differences in their ribonucleolytic activity and conformational stability (Table 1), strongly suggest a role for cationic residues in the internalization process. To delineate which step in the internalization process was being affected by the changes in positive charge, we attempted to observe endocytosis into live cells.

The relative endocytosis of selected ONC variants was observed by flow cytometry using a fluorogenic label that is activated by esterases within the endocytic pathway (Fig. 3). Because cellular binding is a prerequisite for endocytosis, our flow cytometry assay also reports on that pre-equilibrium [63]. We observed that the endocytosis of labeled R15A/K55A/K76A and R15A/K80A/K81A ONC, whose IC_{50} values differ by > 10-fold, differs by just twofold. Thus, R15A/K55A/K76A ONC enters endosomes twice as readily as does R15A/K80A/K81A ONC, which likely accounts for only a small portion of the difference in cytotoxicity. The endocytosis of labeled R15A/K81A did not differ significantly from that of labeled K49A/R73A, even though the IC_{50} values of the two variants differ by 10-fold.

In addition to the variants that were derived from the patches of positive charge on ONC, a variant in which the two active-site lysine residues [34] were replaced with alanine, K9A/K31A ONC, was analyzed for its ability to enter cells by using flow cytometry (Fig. 3C). It has been proposed that the active site of ribonucleases might play a special role in their internalization, based on several observations. Computational analysis on RNase A revealed that the maximal electrostatic interaction energy between the protein and a negatively charged surface occurs with the active site of RNase A facing that surface [66]. In addition, glycosaminoglycans, such as heparan sulfate, are similar to single-stranded nucleic acids in being highly anionic polymers. Indeed, anti-heparin IgM binds to single-stranded DNA and anti-DNA serum binds to heparan sulfate, and heparin affinity chromatography has been used to purify DNA-binding proteins [67,68]. It was thought that the active site of ONC, which binds to RNA and DNA [33,34], might interact with heparan sulfate on the cell surface. Our data, however, show little difference between the endocytosis of labeled wild-type ONC and labeled K9A/K31A ONC, suggesting that these residues are not important for this process.

Potential role of cationic residues in translocation

It is clear from our data that particular cationic surface residues of ONC, especially Lys49 and those in patch 3, play a major role in the cytotoxicity of the protein. That role cannot be accounted for fully by differences in endocytosis (*vide supra*). Our data are consistent with these cationic residues instead mediating the translocation step of ONC. We are able to measure the sum of all of the steps of cytotoxicity (Fig. 4); binding and endocytosis are measured in the flow cytometric assay, and ribonucleolytic activity is measured as an isolated step in an *in vitro* assay. After ruling out effects on all steps other than translocation, we infer that patch 3 and Lys49 are likely mediators of the translocation of ONC across the lipid bilayer.

Translocation is the most mysterious step in the mechanism of ONC-induced cytotoxicity. The acidification of endosomes is not required for translocation

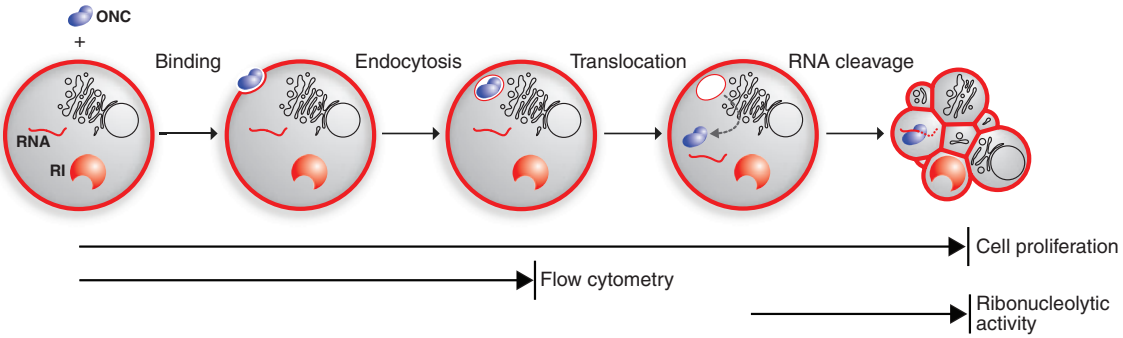

Fig. 4. Putative mechanism for the cytotoxicity of ribonucleases and related assays. Assays of cell proliferation report on the sum of four steps: binding, endocytosis, translocation and RNA cleavage. Assays using flow cytometry and a fluorogenic label report on the first two steps, whereas assays of catalytic activity report on only the final step. Observed differences in the cell proliferation of ONC variants cannot be accounted for by flow cytometry or catalytic activity assays, indicting the translocation step as the differentiating one.

[48,50], and, indeed, neutralization of endosomes increases translocation [55]. A correlation between the ability of dimeric variants of RNase A to disrupt membranes *in vitro*, and their ability to kill cancer cells has led to the hypothesis that the endocytic membrane is disrupted in the translocation process [57]. Our data are consistent with this hypothesis. Specific regions of positive charge have been shown to play a role in the ability of members of the RNase A superfamily to disrupt cell membranes. Human eosinophilic cationic protein (RNase 3) [69] and human ribonuclease 7 (RNase 7) [70] both exhibit bactericidal activity that is thought to proceed via pore formation followed by membrane disruption, similar to the actions of antimicrobial peptides [71]. Certain basic and aromatic residues of eosinophilic cationic protein have been shown to be essential for membrane disruption and bactericidal activity, the net charge or hydrophobicity being less important [72]. Similarly, replacement of clusters of lysine residues on RNase 7 with uncharged residues revealed that only a cluster located near the N-terminus was important for membrane permeability and antimicrobial activity [73]. Work is ongoing in our laboratory to exploit the TML strategy for the direct observation of membrane translocation in live human cells [74].

Conclusions

ONC represents a new class of cancer chemotherapeutic agent – the cytotoxic ribonucleases. ONC is unique in being a natural product and a potential biopharmaceutical agent that is endowed with the ability to cross a cellular membrane and specifically kill cancer cells. Chemical cationization has been shown to increase the cytotoxic ability of ribonucleases, and even endow nontoxic ribonucleases with the ability to kill cells. We have discovered, however, that the net charge of ONC is less important than the distribution of that charge. Although ONC does not interact with the surface of cancer cells through a specific receptor, certain regions of ONC (specifically, residues 49, 73, 76 and 78) appear to be more important than others in the lipid-bilayer translocation step that is required for the cytotoxicity of ONC. These findings provide insight into cytosolic entry, a poorly understood process in the cytotoxicity of ONC and other ribonucleases.

Experimental procedures

Materials

K-562 cells were derived from a continuous human chronic myelogenous leukemia cell line, and obtained from American Type Culture Collection (Manassas, VA, USA). *Escherichia coli* BL21(DE3) cells and pET22b(+) plasmid were from Novagen (Madison, WI, USA).

Enzymes were obtained from Promega (Madison, WI, USA). 6-Carboxyfluorescein–dArUdGdA–6-carboxytetramethylrhodamine (6-FAM–dArUdGdA–6-TAMRA) [33,75] was obtained from Integrated DNA Technologies (Coralville, IA, USA). Cell culture medium and supplements were from Invitrogen (Carlsbad, CA, USA). [*methyl*-^{3}H]Thymidine (6.7 Ci·mmol^{-1}) was from Perkin–Elmer (Boston, MA, USA). Mes buffer (Sigma Aldrich, St Louis, MO, USA) was purified by anion-exchange chromatography to remove oligo(vinylsulfonic acid), a potent inhibitor of ribonucleases [76]. All other chemicals used were of commercial grade or better, and were used without further purification.

Analytical instruments

Molecular mass was measured by MALDI–TOF MS using a Voyager-DE-PRO Biospectrometry Workstation (Applied Biosystems, Foster City, CA, USA). Fluorescence measurements were made with a QuantaMaster1 photon-counting fluorometer equipped with sample stirring (Photon Technology International, South Brunswick, NJ, USA). CD experiments were performed in the University of Wisconsin–Madison Biophysics Instrumentation Facility with a model 62A DS CD spectrophotometer equipped with a temperature controller (Aviv, Lakewood, NJ, USA). Radioactivity was quantified by scintillation counting using a Microbeta TriLux liquid scintillation counter (Perkin–Elmer, Wellesley, MA, USA). Flow cytometry data were collected in the University of Wisconsin Paul P. Carbone Comprehensive Cancer Center with a FACSCalibur flow cytometer equipped with a 488-nm argon-ion laser (Becton Dickinson, Franklin Lakes, NJ, USA).

Production of ribonucleases

DNA encoding ONC variants was created with the plasmid pONC [33] and the Quikchange site-directed mutagenesis kit (Strategene, La Jolla, CA, USA). Wild-type RNase A was purified as described previously [37]. ONC variants were also purified as described previously [37], but with the following exceptions. ONC variants were refolded overnight at room temperature following slow dilution (by 10-fold) into 0.10 M Tris/HCl buffer, pH 8.0, containing NaCl (0.10 M), reduced glutathione (3.0 mM) and oxidized glutathione (0.6 mM). Following concentration by ultrafiltration, samples were dialyzed overnight versus 50 mM sodium acetate buffer, pH 5.0, containing NaCl (0.10 M), and applied to a MonoS cation-exchange FPLC column (Pharmacia, Biotech, Uppsala, Sweden). ONC variants were eluted from the column with a linear gradient of NaCl (0.15–0.3 M) in 50 mM sodium acetate buffer, pH 5.0. The eluate exhibited two peaks at 280 nm, the first of which was from a protein with a pyroglutamate residue at its N-terminus (lower *Z*

value). We used that protein in all of our experiments. If additional protein was needed for a particular experiment, we dialyzed the protein from the second peak against NaCl/P_i to allow the N-terminal glutamine residue to form pyroglutamate (which is a spontaneous process) [77–79], and repeated the cation-exchange chromatography. Protein concentrations were determined by UV spectroscopy using extinction coefficients of $\varepsilon_{280} = 0.87\ (mg{\cdot}mL^{-1})^{-1}{\cdot}cm^{-1}$ for ONC and its variants, and $\varepsilon_{278} = 0.72\ (mg{\cdot}mL^{-1})^{-1}{\cdot}cm^{-1}$ for RNase A [37].

Production of labeled ONC variants

Variants of ONC with a free cysteine at position 61 were protected by reaction with 5,5′-dithio-bis(2-nitrobenzoic acid) [62,80] following gel-filtration chromatography, then dialyzed overnight versus 20 mM sodium acetate buffer, pH 5.0. Samples were applied to a MonoS cation-exchange column, as described above. Prior to attachment of the fluorogenic label, thionitrobenzoic acid-protected ONC variants were deprotected with a fivefold molar excess of dithiothreitol, then desalted by using a PD-10 desalting column (GE Biosciences, Piscataway, NJ, USA). The maleimide-containing fluorogenic label was synthesized as described previously [62]. Deprotected proteins were reacted for 4–6 h at 25 °C with a 10-fold excess of the fluorogenic label. Conjugates were purified by using a HiTrap SP HP column (GE Biosciences, Piscataway, NJ, USA). Concentrations of conjugates were determined with a bicinchoninic acid assay kit from Pierce (Rockford, IL, USA) with BSA as a standard.

Measurements of conformational stability

Conformational stability of wild-type ONC and its variants was determined by CD spectroscopy, as described previously [33], with the following modifications. A solution of ONC ($0.2\ mg{\cdot}mL^{-1}$) in NaCl/P_i was heated from 55 to 99 °C in 2 °C increments, and the molar ellipticity at 204 or 209 nm was monitored following a 5-min equilibration at each temperature. The molar ellipticity data were fitted to a two-state model for denaturation to determine T_m values [81].

Assays of catalytic activity

Ribonucleolytic activity of ONC and its variants was measured by using a hypersensitive fluorogenic substrate, 6-FAM–dArUdGdA–6-TAMRA, as described previously [33,75]. Briefly, fluorescence increase at 515 nm (following excitation at 492 nm) in the presence of ONC and its variants was measured in 0.10 M Mes/NaOH [oligo(vinylsulfonic acid)-free] buffer, pH 6.0, containing NaCl (0.10 M), 6-FAM–dArUdGdA–6-TAMRA (50 nm) and human ribonuclease inhibitor (1 nm) at 23 ± 2 °C. This pH value is close to the pH optimum for catalysis by ONC [34]. Values of k_{cat}/K_M were calculated with the equation:

$$k_{cat}/K_M = \left(\frac{\Delta I/\Delta t}{I_{max} - I_0}\right)\frac{1}{[\text{ribonuclease}]} \quad (1)$$

where $\Delta I/\Delta t$ represents the initial reaction velocity, I_{max} is the fluorescence following complete cleavage of the substrate by excess RNase A, and I_0 is the fluorescence prior to addition of ribonuclease.

Assays of cytotoxicity

K-562 and other mammalian cells exposed to cytotoxic ribonucleases die in an apoptotic manner, and assays of cell proliferation report on the cytotoxic activity of ribonucleases [27–29]. The effect of ONC, its variants and RNase A on the proliferation of K-562 cells was measured by monitoring the incorporation of [*methyl*-^{3}H]thymidine into cellular DNA, as described previously [33]. Experiments were repeated three times in triplicate. Values for IC_{50} were determined by fitting the curves by nonlinear regression to the following equation:

$$y = \frac{100\%}{1 + 10^{(\log(IC_{50}) - \log[\text{ribonuclease}])h}} \quad (2)$$

In Eqn (2), y is the total DNA synthesis following the [*methyl*-^{3}H]thymidine pulse, and h is the slope of the curve.

Flow cytometry

The fluorogenic label is optically silent until it encounters an intracellular esterase. Internalization of ONC variants conjugated to the fluorogenic label was followed by monitoring the increase in fluorescence, as described previously [63]. Briefly, K-562 cells at near-confluency were collected by centrifugation and resuspended at a density of $1 \times 10^6\ cells{\cdot}mL^{-1}$ in RPMI 1640 medium. Labeled or unlabeled ONC (10 μM final concentration) was added to 250 μL of these cells, which were then incubated for varying times at 37 °C. To stop internalization, cells were placed on ice, then collected by centrifugation and resuspended in ice-cold NaCl/P_i. Cells were kept on ice until analysis by flow cytometry.

Fluorescence was detected with a 530/30-nm band-pass filter. Cell viability was determined by staining with propidium iodide, detected with a 660-nm long-pass filter. The mean channel fluorescence intensity of 10 000 or 20 000 viable cells was determined with WINLIST software (Verity Software House, Topsham, ME, USA).

Acknowledgements

We are grateful to J. Puchalski for assistance with the analysis of flow cytometry data, and R. J. Johnson, T. J. Rutkoski, K. L. Gorres, M. N. Levine, J. E. Lee,

M. T. Borra, T.-Y. Chao and G. A. Ellis for contributive discussions. This work was supported by grant CA073808 (NIH). RFT was supported by a Wisconsin Distinguished Rath Graduate Fellowship. LDL was supported by Biotechnology Training Grant 08349 (NIH) and an ACS Division of Organic Chemistry Graduate Fellowship sponsored by the Genentech Foundation. The University of Wisconsin–Madison Biophysics Instrumentation Facility was established with grants BIR-9512577 (NSF) and RR13790 (NIH).

References

1 Raines RT (1998) Ribonuclease A. *Chem Rev* **98**, 1045–1065.
2 Marshall GR, Feng JA & Kuster DJ (2008) Back to the future: ribonuclease A. *Biopolymers* **90**, 259–277.
3 Matoušek J (2001) Ribonucleases and their antitumor activity. *Comp Biochem Physiol* **129C**, 175–191.
4 Leland PA & Raines RT (2001) Cancer chemotherapy – ribonucleases to the rescue. *Chem Biol* **8**, 405–413.
5 Makarov AA & Ilinskaya ON (2003) Cytotoxic ribonucleases: molecular weapons and their targets. *FEBS Lett* **540**, 15–20.
6 Benito A, Ribó M & Vilanova M (2005) On the track of antitumor ribonucleases. *Mol Biosyst* **1**, 294–302.
7 Arnold U & Ulbrich-Hofmann R (2006) Natural and engineered ribonucleases as potential cancer therapeutics. *Biotechnol Lett* **28**, 1615–1622.
8 Arnold U (2008) Aspects of the cytotoxic action of ribonucleases. *Curr Pharm Biotechnol* **9**, 161–168.
9 Ardelt W, Mikulski SM & Shogen K (1991) Amino acid sequence of an anti-tumor protein from *Rana pipiens* oocytes and early embryos. *J Biol Chem* **266**, 245–251.
10 Kim J-S, Souček J, Matoušek J & Raines RT (1995) Catalytic activity of bovine seminal ribonuclease is essential for its immunosuppressive and other biological activities. *Biochem J* **308**, 547–550.
11 Dickson KA, Haigis MC & Raines RT (2005) Ribonuclease inhibitor: structure and function. *Prog Nucleic Acid Res Mol Biol* **80**, 349–374.
12 Lee FS, Shapiro R & Vallee BL (1989) Tight-binding inhibition of angiogenin and ribonuclease A by placental ribonuclease inhibitor. *Biochemistry* **28**, 225–230.
13 Vicentini AM, Kieffer B, Mathies R, Meyhack B, Hemmings BA, Stone SR & Hofsteenge J (1990) Protein chemical and kinetic characterization of recombinant porcine ribonuclease inhibitor expressed in *Saccharomyces cerevisiae*. *Biochemistry* **29**, 8827–8834.
14 Johnson RJ, McCoy JG, Bingman CA, Phillips GN Jr & Raines RT (2007) Inhibition of human pancreatic ribonuclease by the human ribonuclease inhibitor protein. *J Mol Biol* **367**, 434–449.
15 Johnson RJ, Lavis LD & Raines RT (2007) Intraspecies regulation of ribonucleolytic activity. *Biochemistry* **46**, 13131–13140.
16 Leland PA, Staniszewski KE, Kim B-M & Raines RT (2000) A synapomorphic disulfide bond is critical for the conformational stability and cytotoxicity of an amphibian ribonuclease. *FEBS Lett* **477**, 203–207.
17 Klink TA & Raines RT (2000) Conformational stability is a determinant of ribonuclease A cytotoxicity. *J Biol Chem* **275**, 17463–17467.
18 Kim B-M, Kim H, Raines RT & Lee Y (2004) Glycosylation of onconase increases its conformational stability and toxicity for cancer cells. *Biochem Biophys Res Commun* **315**, 976–983.
19 Arnold U, Schulenburg C, Schmidt D & Ulbrich-Hofmann R (2006) Contribution of structural peculiarities of onconase to its high stability and folding kinetics. *Biochemistry* **45**, 3580–3587.
20 Leich F, Stöhr N, Rietz A, Ulbrich-Hofmann R & Arnold U (2007) Endocytotic internalization as a crucial factor for the cytotoxicity of ribonucleases. *J Biol Chem* **282**, 27640–27646.
21 Ilinskaya ON & Makarov AA (2005) Why ribonucleases induce tumor cell death. *Mol Biol* **39**, 1–10.
22 Futami J & Yamada H (2008) Design of cytotoxic ribonucleases by cationization to enhance intracellular protein delivery. *Curr Pharm Biotechnol* **9**, 180–184.
23 Lee JE & Raines RT (2008) Ribonucleases as novel chemotherapeutics: the ranpirnase example. *BioDrugs* **22**, 53–58.
24 Ardelt W, Shogen K & Darzynkiewicz Z (2008) Onconase and Amphinase, the antitumor ribonucleases from *Rana pipiens* oocytes. *Curr Pharm Biotechnol* **9**, 215–225.
25 Darzynkiewicz Z, Carter SP, Mikulski SM, Ardelt WJ & Shogen K (1988) Cytostatic and cytotoxic effect of Pannon (P-30 protein), a novel anticancer agent. *Cell Tissue Kinet* **21**, 169–182.
26 Mikulski SM, Ardelt W, Shogen K, Bernstein EH & Menduke H (1990) Striking increase of survival of mice bearing M109 Madison carcinoma treated with a novel protein from amphibian embryos. *J Natl Cancer Inst* **82**, 151–153.
27 Iordanov MS, Ryabinina OP, Wong J, Dinh TH, Newton DL, Rybak SM & Magun BE (2000) Molecular determinants of apoptosis induced by the cytotoxic ribonuclease onconase: evidence for cytotoxic mechanisms different from inhibition of protein synthesis. *Cancer Res* **60**, 1983–1994.
28 Leland PA, Staniszewski KE, Kim B-M & Raines RT (2001) Endowing human pancreatic ribonuclease with toxicity for cancer cells. *J Biol Chem* **276**, 43095–43102.
29 Grabarek J, Ardelt B, Du L & Darzynkiewicz Z (2002) Activation of caspases and serine proteases during

apoptosis induced by onconase (Ranpirnase). *Exp Cell Res* **278**, 61–71.
30 Costanzi J, Sidransky D, Navon A & Goldsweig H (2005) Ribonucleases as a novel pro-apoptotic anticancer strategy: review of the preclinical and clinical data for ranpirnase. *Cancer Invest* **23**, 643–650.
31 Pavlakis N & Vogelzang NJ (2006) Ranpirnase – an antitumour ribonuclease: its potential role in malignant mesothelioma. *Expert Opin Biol Ther* **6**, 391–399.
32 Halicka DH, Pozarowski P, Ita M, Ardelt WJ, Mikulski SM, Shogen K & Darzynkiewicz Z (2002) Enhancement of activation-induced apoptosis of lymphocytes by the cytotoxic ribonuclease onconase (Ranpirnase). *Int J Oncol* **21**, 1245–1250.
33 Lee JE & Raines RT (2003) Contribution of active-site residues to the function of onconase, a ribonuclease with antitumoral activity. *Biochemistry* **42**, 11443–11450.
34 Lee JE, Bae E, Bingman CA, Phillips GN Jr & Raines RT (2008) Structural basis for catalysis by onconase. *J Mol Biol* **374**, 165–177.
35 Boix E, Wu Y, Vasandani VM, Saxena SK, Ardelt W, Ladner J & Youle RJ (1996) Role of the N-terminus in RNase A homologues: differences in catalytic activity, ribonuclease inhibitor interaction and cytotoxicity. *J Mol Biol* **257**, 992–1007.
36 Turcotte RF & Raines RT (2008) Interaction of onconase with the ribonuclease inhibitor protein. *Biochem Biophys Res Commun* **377**, 512–514.
37 Leland PA, Schultz LW, Kim B-M & Raines RT (1998) Ribonuclease A variants with potent cytotoxic activity. *Proc Natl Acad Sci USA* **98**, 10407–10412.
38 Fisher BM, Ha J-H & Raines RT (1998) Coulombic forces in protein–RNA interactions: binding and cleavage by ribonuclease A and variants at Lys7, Arg10 and Lys66. *Biochemistry* **37**, 12121–12132.
39 Fisher BM, Schultz LW & Raines RT (1998) Coulombic effects of remote subsites on the active site of ribonuclease A. *Biochemistry* **37**, 17386–17401.
40 Fisher BM, Grilley JE & Raines RT (1998) A new remote subsite in ribonuclease A. *J Biol Chem* **273**, 34134–34138.
41 Park C & Raines RT (2001) Quantitative analysis of the effect of salt concentration on enzymatic catalysis. *J Am Chem Soc* **123**, 11472–11479.
42 Futami J, Maeda T, Kitazoe M, Nukui E, Tada H, Seno M, Kosaka M & Yamada H (2001) Preparation of potent cytotoxic ribonucleases by cationization: enhanced cellular uptake and decreased interaction with ribonuclease inhibitor by chemical modification of carboxyl groups. *Biochemistry* **26**, 7518–7524.
43 Fuchs SM, Rutkoski TJ, Kung VM, Groeschl RT & Raines RT (2007) Increasing the potency of a cytotoxin with an arginine graft. *Protein Eng Des Sel* **20**, 505–509.
44 Smith MR, Newton DL, Mikulski SM & Rybak SM (1999) Cell cycle-related differences in susceptibility of NIH/3T3 cells to ribonucleases. *Exp Cell Res* **247**, 220–232.
45 Newton DL, Hansen HJ, Mikulski SM, Goldenberg DM & Rybak SM (2001) Potent and specific antitumor effects of an anti-CD22-targeted cytotoxic ribonuclease: potential for the treatment of non-Hodgkin lymphoma. *Blood* **97**, 528–535.
46 De Lorenzo C & D'Alessio G (2008) From immunotoxins to immunoRNases. *Curr Pharm Biotechnol* **9**, 210–214.
47 Sandvig K, Spilsberg B, Lauvrak SU, Torgersen ML, Iversen TG & van Deurs B (2004) Pathways followed by protein toxins into cells. *Int J Med Microbiol* **293**, 483–490.
48 Wu Y, Mikulski SM, Ardelt W, Rybak SM & Youle RJ (1993) A cytotoxic ribonuclease. Study of the mechanism of onconase cytotoxicity. *J Biol Chem* **268**, 10686–10693.
49 Wu Y, Saxena SK, Ardelt W, Gadina M, Mikulski SM, De Lorenzo V, D'Alessio G & Youle RJ (1995) A study of the intracellular routing of cytotoxic ribonucleases. *J Biol Chem* **270**, 17476–17481.
50 Haigis MC & Raines RT (2003) Secretory ribonucleases are internalized by a dynamin-independent endocytic pathway. *J Cell Sci* **116**, 313–324.
51 Sasisekharan R, Shriver Z, Venkataraman G & Narayanasami U (2002) Roles of heparan-sulphate glycosaminoglycans in cancer. *Nat Rev Cancer* **2**, 521–528.
52 Bergelson LD, Dyatlovitskaya EV, Torkhovskaya TI, Sorokina IB & Gorkova NP (1970) Phospholipid composition of membranes in the tumor cell. *Biochim Biophys Acta* **210**, 287–298.
53 Ran S, Downes A & Thorpe PE (2002) Increased exposure of anionic phospholipids on the surface of tumor blood vessels. *Cancer Res* **62**, 6132–6140.
54 Fredman P, Hedberg K & Brezicka T (2003) Gangliosides as therapeutic targets for cancer. *BioDrugs* **17**, 155–167.
55 Rodriguez M, Torrent G, Bosch M, Rayne F, Dubremetz J-F, Ribó M, Benito A, Vilanova M & Beaumelle B (2007) Intracellular pathway of Onconase that enables its delivery to the cytosol. *J Cell Sci* **120**, 1405–1411.
56 Ilinskaya ON, Dreyer F, Mitkevich VA, Shaw KL, Pace CN & Makarov AA (2002) Changing the net charge from negative to positive makes ribonuclease Sa cytotoxic. *Protein Sci* **11**, 2522–2525.
57 Notomista E, Mancheño JM, Crescenzi O, Di Donato A, Gavilanes J & D'Alessio G (2006) The role of electrostatic interactions in the antitumor activity of dimeric RNases. *FEBS J* **273**, 3687–3697.
58 Fuchs SM & Raines RT (2005) Polyarginine as a multifunctional fusion tag. *Protein Sci* **14**, 1538–1544.

59 Futami J, Nukui K, Maeda T, Kosaka M, Tada H, Seno M & Yamada H (2002) Optimum modification for the highest cytotoxicity of cationized ribonuclease. *J Biochem (Tokyo)* **132**, 223–228.
60 Schulenburg C, Ardelt B, Ardelt W, Arnold U, Shogen K, Ulbrich-Hofmann R & Darzynkiewicz Z (2007) The interdependence between catalytic activity, conformational stability, and cytotoxicity of onconase. *Cancer Biol Ther* **6**, 1233–1239.
61 Knowles JR (1987) Tinkering with enzymes: what are we learning? *Science* **236**, 1252–1258.
62 Lavis LD, Chao T-Y & Raines RT (2006) Fluorogenic label for biomolecular imaging. *ACS Chem Biol* **1**, 252–260.
63 Johnson RJ, Chao T-Y, Lavis LD & Raines RT (2007) Cytotoxic ribonucleases: the dichotomy of Coulombic forces. *Biochemistry* **46**, 10308–10316.
64 Saxena SK, Rybak SM, Winkler G, Meade HM, McGray P, Youle RJ & Ackerman EJ (1991) Comparison of RNases and toxins upon injection into *Xenopus* oocytes. *J Biol Chem* **266**, 21208–21214.
65 Suhasini AN & Sirdeshmukh R (2006) Transfer RNA cleavages by onconase reveal unusual cleavage sites. *J Biol Chem* **281**, 12201–12209.
66 Yoon BJ & Lenhoff AM (1992) Computation of the electrostatic interaction energy between a protein and a charged surface. *J Phys Chem* **96**, 3130–3134.
67 Faaber P, Rijke TP, van de Putte LB, Capel PJ & Berden JH (1986) Cross-reactivity of human and murine anti-DNA antibodies with heparan sulfate. The major glycosaminoglycan in glomerular basement membranes. *J Clin Invest* **77**, 1824–1830.
68 Belting M (2003) Heparan sulfate proteoglycan as a plasma membrane carrier. *Trends Biochem Sci* **28**, 145–151.
69 Lehrer RI, Szklarek D, Barton A, Ganz T, Hamann KJ & Gleich GJ (1989) Antibacterial properties of eosinophil major basic protein and eosinophil cationic protein. *J Immunol* **142**, 4428–4434.
70 Zhang J, Dyer KD & Rosenberg HF (2003) Human RNase 7: a new cationic ribonuclease of the RNase A superfamily. *Nucleic Acids Res* **31**, 602–607.
71 Henriques ST, Melo MN & Castanho MA (2006) Cell-penetrating peptides and antimicrobial peptides: how different are they? *Biochem J* **399**, 1–7.
72 Carreras E, Boix E, Rosenberg HF, Cuchillo CM & Nogues MV (2003) Both aromatic and cationic residues contribute to the membrane-lytic and bactericidal activity of eosinophil cationic protein. *Biochemistry* **42**, 6636–6644.
73 Huang YC, Lin YM, Chang TW, Wu SJ, Lee YS, Chang MD, Chen C, Wu SH & Liao YD (2007) The flexible and clustered lysine residues of human ribonuclease 7 are critical for membrane permeability and antimicrobial activity. *J Biol Chem* **282**, 4626–4633.
74 Lavis LD & Raines RT (2008) Bright ideas for chemical biology. *ACS Chem Biol* **3**, 142–155.
75 Kelemen BR, Klink TA, Behlke MA, Eubanks SR, Leland PA & Raines RT (1999) Hypersensitive substrate for ribonucleases. *Nucleic Acids Res* **27**, 3696–3701.
76 Smith BD, Soellner MB & Raines RT (2003) Potent inhibition of ribonuclease A by oligo(vinylsulfonic acid). *J Biol Chem* **278**, 20934–20938.
77 Blombäck B (1967) Derivatives of glutamine in peptides. *Methods Enzymol* **11**, 398–411.
78 Ribó M, Bosch M, Torrent G, Benito A, Beaumelle B & Vilanova M (2004) Quantitative analysis, using MALDI-TOF mass spectrometry, of the N-terminal hydrolysis and cyclization reactions of the activation process of onconase. *Eur J Biochem* **271**, 1163–1171.
79 Welker E, Hathaway L, Xu G, Narayan M, Pradeep L, Shin HC & Scheraga HA (2007) Oxidative folding and N-terminal cyclization of onconase. *Biochemistry* **46**, 5485–5493.
80 Riddles PW, Blakeley RL & Zerner B (1983) Reassessment of Ellman's reagent. *Methods Enzymol* **91**, 49–60.
81 Pace CN & Scholtz JM (1997) Measuring the conformational stability of a protein. In *Protein Structure*, 2nd edn. (Creighton TE, ed.), pp. 299–321. Oxford University Press, New York.
82 Mosimann SC, Ardelt W & James MNG (1994) Refined 1.7 Å X-ray crystallographic structure of P-30 protein, an amphibian ribonuclease with anti-tumor activity. *J Mol Biol* **236**, 1141–1153.

Supporting information

The following supplementary material is available:

Fig. S1. Effect of ONC triple variants on the proliferation of K-562 cells.

Fig. S2. Effect of ONC double variants on the proliferation of K-562 cells.

Table S1. Mass analysis of ONC and its variants.

This supplementary material can be found in the online version of this article.

Please note: As a service to our authors and readers, this journal provides supporting information supplied by the authors. Such materials are peer-reviewed and may be re-organized for online delivery, but are not copy-edited or typeset. Technical support issues arising from supporting information (other than missing files) should be addressed to the authors.